J|A|C|S
ARTICLES

Published on Web 03/20/2009

Kinetics of Silica Nucleation on Carboxyl- and Amine-Terminated Surfaces: Insights for Biomineralization

Adam F. Wallace,* James J. DeYoreo,† and Patricia M. Dove

Department of Geosciences, Virginia Polytechnic Institute & State University, Blacksburg, Virginia 24061

Received December 4, 2008; E-mail: afw@vt.edu

Abstract: An in situ, atomic force microscopy- (AFM-)-based experimental approach is developed to directly measure the kinetics of silica nucleation on model biosubstrates under chemical conditions that mimic natural biosilica deposition environments. Relative contributions of thermodynamic and kinetic drivers to surface nucleation are quantified by use of amine-, carboxyl-, and hybrid NH_3^+/COO^--terminated surfaces as surrogates for charged and ionizable groups on silica-mineralizing organic matrices. The data show that amine-terminated surfaces do not promote silica nucleation, whereas carboxyl and hybrid NH_3^+/COO^- substrates are active for silica deposition. The rate of silica nucleation is $\sim 18\times$ faster on the hybrid substrates than on carboxylated surfaces, but the free energy barriers to cluster formation are similar on both surface types. These findings suggest that surface nucleation rates are more sensitive to kinetic drivers than previously believed and that cooperative interactions between oppositely charged surface species play important roles in directing the onset of silica nucleation. Further experiments to test the importance of these cooperative interactions with patterned NH_3^+/COO^- substrates, and aminated surfaces with solution-borne anionic species, confirm that silica nucleation is most rapid when oppositely charged species are proximal. By documenting the synergy that occurs between surface groups during silica formation, these findings demonstrate a new type of emergent behavior underlying the ability of self-assembled molecular templates to direct mineral formation.

Introduction

Understanding the processes by which biomolecules direct the formation of mineralized tissues and skeletal components within living organisms is a central challenge of the biomineralization community. Recent efforts in this area are turning toward silicifying species, whose biologically controlled routes to silica formation are consequential to biomimetic materials design and nanotechnology development.[1,2] Among the most widely studied silica mineralizing organisms (e.g., diatoms, radiolaria, sponges), the diatoms exert the greatest influence over global biogeochemical processes. As prominent members of phytoplankton assemblages in marine environments, diatoms suppress the concentration of aqueous silicate in modern oceans to levels far below saturation with respect to amorphous silica,[3−5] and account for ∼40% of primary biological production in the oceans.[6,7]

Until recently, physical models for silica biomineralization in diatoms and sponges were derived largely from macroscopic investigations,[8−17] which provided ample information about the hierarchical organization of naturally occurring biosilica structures but limited insights into the chemical basis of biosilica deposition. With the advent of modern biochemical probes, pioneering studies are now yielding chemical and structural information about the macromolecular species that may facilitate formation of siliceous skeletons in vivo. Specialized proteins (silaffins, silacidins, silicateins) and long-chain polyamines

† Present address: Molecular Foundry, Lawrence Berkeley National Laboratory, Berkeley, CA 94720.

(1) Hildebrand, M. *J. Nanosci. Nanotechnol.* **2005**, *5*, 146–157.
(2) Gebeshuber, L. C. *Nano Today* **2007**, *2*, 30–37.
(3) Smetacek, V. *Protist* **1999**, *150*, 25–32.
(4) Racki, G.; Cordey, F. *Earth-Sci. Rev.* **2000**, *52*, 83–120.
(5) Ragueneau, O.; Treguer, P.; Leynaert, A.; Anderson, R. F.; Brzezinski, M. A.; DeMaster, D. J.; Dugdale, R. C.; Dymond, J.; Fischer, G.; Francois, R.; Heinze, C.; Maier-Reimer, E.; Martin-Jezequel, V.; Nelson, D. M.; Queguiner, B. *Global Planetary Change* **2000**, *26*, 317–365.
(6) Nelson, D. M.; Treguer, P.; Brzezinski, M. A.; Leynaert, A.; Queguiner, B. *Global Biogeochem. Cycles* **1995**, *9*, 359–372.
(7) Falkowski, P. G.; Barber, R. T.; Smetacek, V. *Science* **1998**, *281*, 200–206.
(8) Volcani, B. E. In *Silicon and Siliceous Structures in Biological Systems*; Simpson, T. L., Volcani, B. E., Eds.; Springer-Verlag: New York, 1981; pp 157−200.
(9) Crawford, R. M. In *Silicon and Siliceous Structures in Biological Systems*; Simpson, T. L., Volcani, B. E., Eds.; Springer-Verlag: New York, 1981; pp 129−156.
(10) Aizenberg, J.; Weaver, J. C.; Thanawala, M. S.; Sundar, V. C.; Morse, D. E.; Fratzl, P. *Science* **2005**, *309*, 275–278.
(11) Gordon, R.; Drum, R. W. *Int. Rev. Cytol.* **1994**, *150*, 243–372.
(12) Garrone, R.; Simpson, T. L.; Pottu-Boumendil, J. In *Silicon and Siliceous Structures in Biological Systems*; Simpson, T. L., Volcani, B. E., Eds.; Springer-Verlag: New York, 1981; pp 495−526.
(13) Crawford, S. A.; Higgins, M. J.; Mulvaney, P.; Wetherbee, R. *J. Phycol.* **2001**, *37*, 543–554.
(14) Round, F. E. In *Silicon and Siliceous Structures in Biological Systems*; Simpson, T. L., Volcani, B. E., Eds.; Springer-Verlag: New York, 1981; pp 97−128.
(15) Li, C. W.; Volcani, B. E. *Philos. Trans. R. Soc. London, Ser. B* **1984**, *304*, 519.
(16) Pickett-Heaps, J.; Schmid, A. M. M.; Edgar, L. A. In *Progress in Phycological Research*; Round, F. E., Chapman, D. J., Eds.; Biopress Ltd.: Bristol, U.K., 1990; Vol. 7, pp 1−168.
(17) Sumper, M.; Brunner, E.; Lehmann, G. *FEBS Lett.* **2005**, *579*, 3765–3769.

10.1021/ja809486b CCC: $40.75

(LCPA) found in association with siliceous diatom frustules and sponge spicules are demonstrated facilitators of silica mineralization ex vivo[18−22] and are thought to initiate and control silica deposition within highly regulated internal environments.

Although these macromolecules have been identified, considerable effort continues to be applied toward understanding the mechanisms through which they initiate silica nucleation. In situ silica precipitation assays with silicon alkoxide precursors to silicic acid and purified silicatein extracts from the glass sponge *Hexactinellida* suggest that a neutral serine amino acid in the protein active site is temporarily ionized by an imidazole group on an adjacent histidine during silica formation.[23−25] Similar assays with diatom macromolecules imply that cationic amine-bearing portions of silaffins and LCPAs interact with negatively charged peptide-bound phosphoryl groups or solution-borne polyanions to induce the formation of a macromolecular assembly that promotes silica deposition.[20,26−29] In both instances the dynamic interplay between adjacent functional groups, charged and ionizable moieties in particular, has an essential role in promoting silica nucleation.

Macromolecular assemblies with specific arrangements of chemical moieties that induce formation of mineral components are commonly referred to as templates. In general, the rate of mineral formation on the template is attributed to local perturbations in interfacial energy that reduce the free energy barriers to nucleation.[30]

Support for this function comes from in vitro studies of calcite nucleation on templates composed of self-assembled alkanethiol monolayers (SAMs) on noble metal substrates.[31,32] In these systems, not only is nucleation enhanced at the SAM surface but also the orientations of the resulting crystals are controlled. In analogy to epitaxial systems, the general assumption is that such control is the result of minimizing the interfacial energy between substrate and overgrowth. But the interfacial free energy only captures the thermodynamic component of the nucleation barrier. Nucleation rates are also controlled by kinetic barriers associated with desolvation, hydrolysis, or other chemical reactions, binding and unbinding events, and in some cases, diffusion.[33,34] To our knowledge, however, there has been no experimental effort to directly measure the contributions of thermodynamic and kinetic drivers to the surface nucleation rate in biomimetic systems.

This study reports findings from an experimental model system that is designed to mimic key features of biosilica deposition environments and to evaluate the extent to which charged biological interfaces promote silica nucleation by modulating thermodynamic and kinetic barriers. Using in situ tapping-mode atomic force microscopy (TM-AFM), we directly measure the influence of both cationic and anionic surface-bound functional groups on the rate of silica nucleation. Analysis of the kinetic data within the constructs of nucleation theory allows both thermodynamic and kinetic drivers of surface nucleation to be quantified. Development of this method for measuring surface nucleation rates was inspired by previous work on protein crystallization[35] and modified for use with amine- and carboxyl-terminated model biosubstrates that are used as surrogates for moieties on silica-mineralizing organic matrices. Under the pH conditions of the rate measurements, aminated and carboxylated surfaces provided cationic and anionic surfaces, respectively. Hybrid surfaces consisting of both amine and carboxyl moieties were used to test for possible cooperative interactions between oppositely charged functional groups.

Two important findings arise from these measurements. First, amine-terminated surfaces are resistant to silica deposition at low driving forces and can be activated for silica nucleation only if anionic species are also present. This observation is consistent with previous investigations but demonstrates for the first time that interactions between oppositely charged moieties directly promote the condensation of silicic acid in addition to directing the self-assembly of the organic matrix (as previously asserted). Further measurements on hybrid carboxyl−amine surfaces showed that cooperative interactions between adjacent cationic and anionic functional groups accelerate nucleation rates through kinetic effects without significantly reducing the energy barrier to nucleation compared with carboxyl surfaces. This second finding challenges the long-held assumption that surface nucleation in matrix-mediated biomineralization systems is driven entirely by a reduction in the free energy barrier to critical cluster formation at the template surface. These in situ measurements support recent work which demonstrates that the choice of nucleation pathway can indeed be dominated by kinetic factors rather than thermodynamic barriers.[36]

Results and Discussion

Carboxyl-Terminated Surfaces. Carboxyl-terminated self-assembled monolayer films have been extensively used in biomineralization studies,[31,32] and under our experimental conditions they provide a reliable source of surface-bound anionic species akin to those implicated in biosilica formation. Nucleation of amorphous silica was observed on carboxylated surfaces at pH $= 5.0 \pm 0.05$, over a range of silicic acid concentrations that are representative of the observed variability in the intracellular silicon pool for a number of diatom species. Supersaturation, or chemical driving force is defined as

(18) Kroger, N.; Deutzmann, R.; Sumper, M. *Science* **1999**, *286*, 1129–1132.
(19) Kroger, N.; Deutzmann, R.; Sumper, M. *J. Biol. Chem.* **2001**, *276*, 26066–26070.
(20) Kroger, N.; Lorenz, S.; Brunner, E.; Sumper, M. *Science* **2002**, *298*, 584–586.
(21) Kroger, N.; Deutzmann, R.; Bergsdorf, C.; Sumper, M. *Proc. Natl. Acad. Sci. U.S.A.* **2000**, *97*, 14133–14138.
(22) Sumper, M.; Lorenz, S.; Brunner, E. *Angew. Chem., Int. Ed.* **2003**, *42*, 5192–5195.
(23) Cha, J. N.; Shimizu, K.; Zhou, Y.; Christiansen, S. C.; Chmelka, B. F.; Stucky, G. D.; Morse, D. E. *Proc. Natl. Acad. Sci. U.S.A.* **1999**, *96*, 361–365.
(24) Zhou, Y.; Shimizu, K.; Cha, J. N.; Stucky, G. D.; Morse, D. E. *Angew. Chem., Int. Ed.* **1999**, *38*, 780–782.
(25) Shimizu, K.; Cha, J.; Stucky, G. D.; Morse, D. E. *Proc. Natl. Acad. Sci. U.S.A.* **1998**, *95*, 6234–6238.
(26) Brunner, E.; Lutz, K.; Sumper, M. *Phys. Chem. Chem. Phys.* **2004**, *6*, 854–857.
(27) Demadis, K. D.; Neofotistou, E. *Chem. Mater.* **2007**, *19*, 581–587.
(28) Sumper, M.; Kroger, N. *J. Mater. Chem.* **2004**, *14*, 2059–2065.
(29) Lutz, K.; Groger, C.; Sumper, M.; Brunner, E. *Phys. Chem. Chem. Phys.* **2005**, *7*, 2812–2815.
(30) Stokes, R. J.; Evans, D. F. *Fundamentals of Interfacial Engineering*; Wiley−VCH: New York, 1997.
(31) Addadi, L.; Moradian, J.; Shay, E.; Maroudas, N. G.; Weiner, S. *Proc. Natl. Acad. Sci. U.S.A.* **1987**, *84*, 2732–2736.
(32) Aizenberg, J.; Black, A. J.; Whitesides, G. M. *Nature* **1999**, *398*, 495–498.
(33) Himawan, C.; Starov, V. M.; Stapley, A. G. F. *Adv. Colloid Interface Sci.* **2006**, *122*, 3–33.
(34) Turnbull, D.; Fisher, J. C. *J. Chem. Phys.* **1949**, *17*, 71–73.
(35) Galkin, O.; Vekilov, P. G. *J. Phys. Chem. B* **1999**, *103*, 10965–10971.
(36) Yau, S. T.; Vekilov, P. G. *J. Am. Chem. Soc.* **2001**, *123*, 1080–1089.

$$\sigma = \ln\left(\frac{[H_4SiO_4]}{K_{sp}}\right) \quad (1)$$

where $[H_4SiO_4]$ is silicic acid concentration (approximately equal to activity for this uncharged species) and K_{sp} is the equilibrium solubility product of amorphous silica ($K_{sp} = 10^{-2.71}$ at 25 °C). Surface nucleation rate experiments were conducted under moderately supersaturated conditions for biomimetic silicification, within the range of $\sigma = 1.86-2.44$. An organic precursor to silicic acid (TMOS) was used to avoid the formation of precondensed solution-borne silicate species prior to surface nucleation, and constant surface nucleation rates were measured within a time window defined by the onset of solution nucleation (see Experimental Section).

The number of amorphous silica nuclei that formed on COO^--terminated surfaces increased linearly with time, and faster nucleation rates were observed in solution with higher supersaturation states, as expected under steady-state conditions (Figure 1). To our knowledge, these are the first direct measurements of silica nucleation rates onto functionalized substrates. At low driving forces ($\sigma < 2.14$), surface nucleation was the dominant process acting to remove silica from solution. Above $\sigma = 2.14$, surface nucleation rates slowed, suggesting that solution-borne processes were becoming a significant precipitation mechanism at higher driving force. Silica clusters were less than 5 nm in height and contacted carboxylated surfaces at 80−100° (see Supporting Information). Figure 2a shows a typical carboxylated surface with circles to highlight nuclei and more clearly illustrate the substrate-dependent density of silica particles at similar times. Although AFM tip convolution caused the silica nuclei to appear many times wider than they actually were, the high value of the silica−substrate contact angle indicated that the silica particles were hemispherical, with radii roughly equal to the cluster height.

Amine-Terminated Surfaces. In contrast to COO^--terminated substrates, the NH_3^+ surfaces failed to induce surface nucleation under identical solution conditions (Figure 2). For these mild growth conditions, aminated surfaces appeared to stabilize silicic acid solutions rather than promote nucleation, which is consistent with the results of Behrens et al.[37] and Demadis and Neofotistou,[27] who showed that polyamines do not directly catalyze silicic acid condensation reactions. However, there are also a number of investigations in the literature that argue (or assume) that polyaminated species have an intrinsic ability to promote silica formation.[18,21,22,28,38−52] A closer look at these studies revealed that they generally employed extreme silica growth conditions where multiple, often competing processes such as surface and solution-borne nucleation, growth, and particle aggregation may have proceeded concurrently. In this situation, the contributions of individual functional groups to surface nucleation versus colloid aggregation processes may be difficult to assess. It is possible that polyaminated compounds used in earlier studies could have acted as solution-borne aggregation centers upon which preformed and negatively charged colloidal silica particles coalesced and ripened.

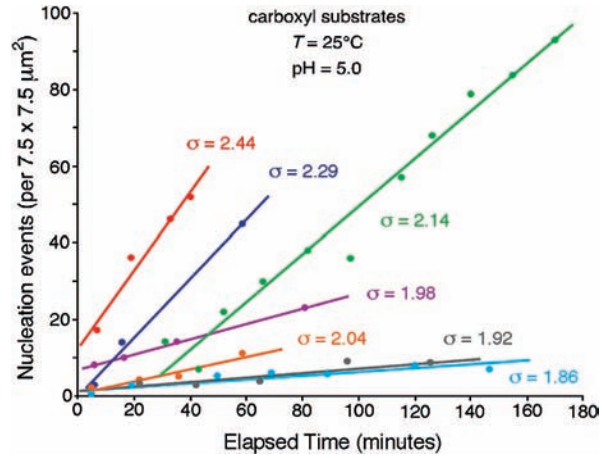

Figure 1. Plot showing linear scaling of surface nucleation events with time and dependence of the nucleation rate (given by slopes of the lines) upon the solution saturation state, σ. All data are for carboxyl-terminated surfaces at pH = 5.0 and $T = 25$ °C. In some instances the regression lines do not pass through the origin because air bubbles present at the outset of these experiments could not be easily distinguished from growing silica nuclei and were included in the total count of nucleation events throughout. These lines are slightly offset, but their slopes are unaffected.

Hybrid Surfaces. Observations from the carboxyl- and amine-terminated surfaces led us to test the hypothesis that the essential role of aminated groups in promoting silica nucleation arises only when a neighboring anionic group is in close proximity. Motivation for examining a synergistic interaction between oppositely charged groups is also found in evidence from the diatoms and glass sponges, where similar relations among charged and ionizable groups have been invoked to provide a mechanistic framework for organosilicate hydrolysis and self-assembly of the organic template.[20,23,24,26,29] To test the idea that similar interactions between cationic and anionic species control the spatial onset of silica nucleation, a hybrid substrate with NH_3^+/COO^- termination was synthesized. Remarkably, these hybrid surfaces were more amenable to silica nucleation than the purely carboxylated and aminated substrates, exhibiting a greater nucleation site density after comparatively less exposure to the growth solution (see Figure 2). As shown later, rates on NH_3^+/COO^- films were up to 18× faster (for $\sigma < 2.14$) than those measured on COO^--terminated films.

(37) Behrens, P.; Jahns, M.; Menzel, H. In *Handbook of Biomineralization*; Behrens, P.; Bauerlein, E., Eds.; Wiley−VCH: Weinheim, Germany, 2007; Vol. 2, pp 3−18.
(38) Belton, D.; Paine, G.; Patwardhan, S. V.; Perry, C. C. *J. Mater. Chem.* **2004**, *14*, 2231–2241.
(39) Belton, D.; Patwardhan, S. V.; Perry, C. C. *Chem. Commun.* **2005**, 3475–3477.
(40) Belton, D. J.; Patwardhan, S. V.; Annenkov, V. V.; Danilovtseva, E. N.; Perry, C. C. *Proc. Natl. Acad. Sci. U.S.A.* **2008**, *105*, 5963–5968.
(41) Coradin, T.; Durupthy, O.; Livage, J. *Langmuir* **2002**, *18*, 2331–2336.
(42) Coradin, T.; Livage, J. *Colloids Surf., B* **2001**, *21*, 329–336.
(43) Delak, K. M.; Sahai, N. *Chem. Mater.* **2005**, *17*, 3221–3227.
(44) Larsen, G.; Lotero, E.; Marquez, M. *J. Phys. Chem. B* **2000**, *104*, 4840–4843.
(45) Patwardhan, S. V.; Clarson, S. J. *Polym. Bull.* **2002**, *48*, 367–371.
(46) Patwardhan, S. V.; Clarson, S. J. *Mater. Sci. Eng., C* **2003**, *23*, 495–499.
(47) Patwardhan, S. V.; Clarson, S. J. *J. Inorg. Organomet. Polym.* **2003**, *13*, 49–53.
(48) Patwardhan, S. V.; Clarson, S. J. *J. Inorg. Organomet. Polym.* **2003**, *13*, 193–203.
(49) Patwardhan, S. V.; Durstock, M. F.; Clarson, S. J. In *Synthesis and Properties of Silicones and Silicone-Modified Materials*; ACS Symposium Series 838; American Chemical Society: Washington, DC, 2003; pp 366−374.
(50) Patwardhan, S. V.; Maheshwari, R.; Mukherjee, N.; Kiick, K. L.; Clarson, S. J. *Biomacromolecules* **2006**, *7*, 491–497.
(51) Patwardhan, S. V.; Mukherjee, N.; Clarson, S. J. *J. Inorg. Organomet. Polym.* **2001**, *11*, 193–198.
(52) Robinson, D. B.; Rognlien, J. L.; Bauer, C. A.; Simmons, B. A. *J. Mater. Chem.* **2007**, *17*, 2113–2119.

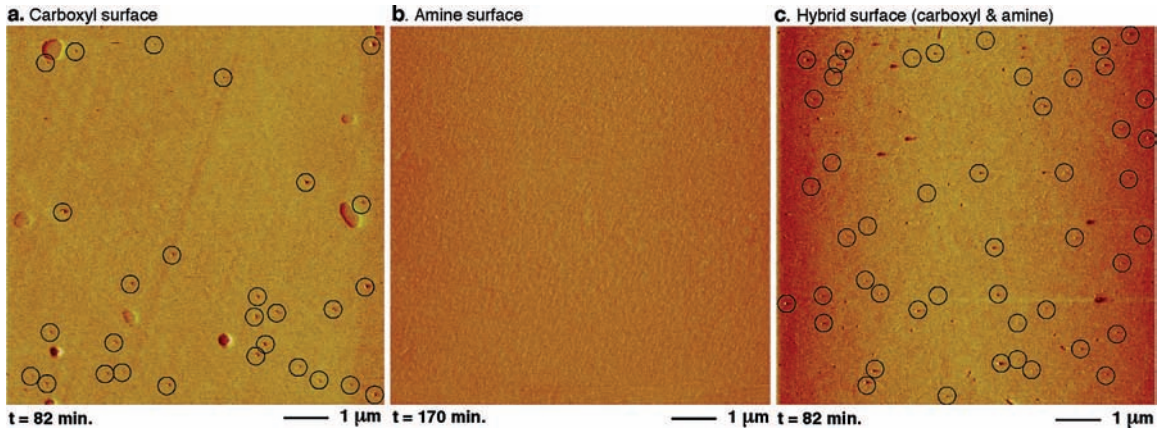

Figure 2. AFM phase images of model substrates during in situ nucleation rate measurements (captured at pH = 5.0, $\sigma = 2.14$, and $T = 25$ °C). Prominent silica particles are highlighted with circles. (a) COOH-terminated surface with silica nuclei at early and late experimental stages. Surface striations and submicrometer pits and islands are features of the underlying Au(111) surface. (b) NH_3^+-terminated surface displaying no evidence of silica deposition nearly 2 h after nuclei were first observed on the carboxylated surfaces. (c) COOH and NH_3^+ surface displaying a greater density of silica nuclei than measured on COOH-terminated surfaces after the same amount of time as in panel a.

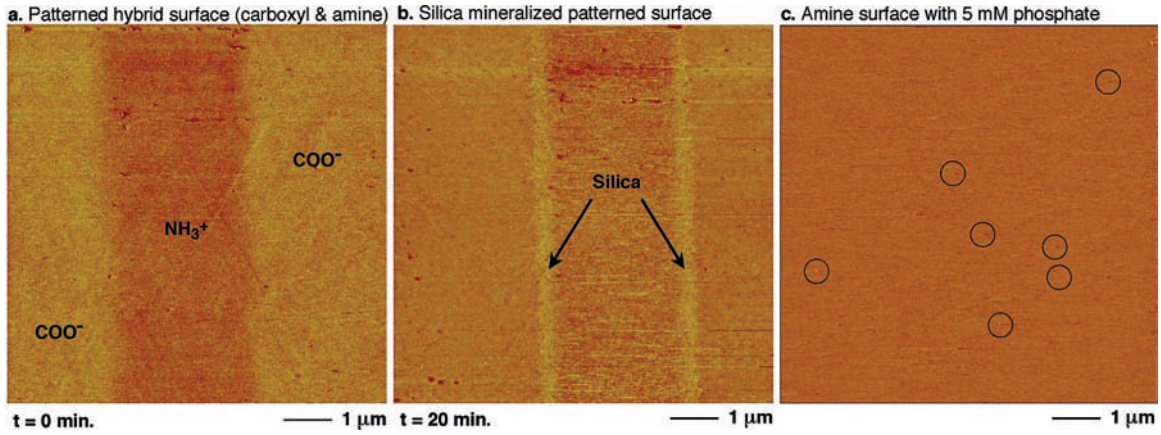

Figure 3. AFM phase images captured at pH = 5.0, $\sigma = 2.14$, and $T = 25$ °C. Patterned substrate with alternating stripes of amine- and carboxyl-terminated areas (a) before and (b) after the introduction of growth solution shows that the onset of silica deposition occurs at NH_3^+/COO^- interface. (c) Amine-terminated surface activated for silica deposition by the presence of 5 mM orthophosphate. Prominent silica particles are highlighted with circles.

Further Tests of Hybrid Nucleation Surfaces. To independently confirm the finding that oppositely charged functional groups promote the formation of amorphous silica through cooperative interactions, we conducted two additional types of nucleation experiments. The first used microcontact lithography to synthesize simple patterned surfaces with bands of carboxyl- and amine-terminated regions (Figure 3a). We conducted flow-through nucleation experiments at controlled supersaturation ($\sigma = 2.14$; pH = 5.0), and AFM observations unambiguously confirmed that the onset of silica deposition was preferentially localized along the intersection between the carboxyl- and amine-terminated areas (Figure 3b). These qualitative observations provide unambiguous support to our finding that nucleation is favored on hybrid NH_3^+/COO^- substrates.

In a second type of experiment we returned to purely aminated surfaces; but this time we provided negatively charged species to the system by adding orthophosphate to the growth solution. In this environment ($\sigma = 2.14$, pH = 5.0, $[PO_4^{3-}] = 5$ mM), silica nuclei indeed formed on the amine-terminated films within 1 h (Figure 3c), albeit at a lower density than observed on either COO^- or NH_3^+/COO^- surfaces after a comparable period of time. In this case the nuclei are easily displaced by the AFM tip, indicating that the interactions between the nuclei and the underlying surface are relatively weak compared to those between silica and the carboxyl, hybrid, and patterned substrates.

Analysis of Kinetic Data. Rate measurements present a unique opportunity to quantify kinetic and thermodynamic origins of substrate-dependent nucleation. The surface nucleation rate is given by[34,53]

$$J_n = A \exp\left(-\frac{\Delta G^*}{k_B T}\right) \quad (2)$$

where J_n = steady-state surface nucleation rate (number of nucleation events per square meter per second), ΔG^* = thermodynamic barrier to forming a critically sized molecular cluster, $k_B T$ = product of Boltzmann constant and system temperature, and A = kinetic constant, whose value depends upon many physical parameters including diffusional and steric barriers.[34,35,53]

Within the constructs of classical nucleation theory, ΔG^* can be expressed in terms of silica supersaturation:

(53) Nielsen, A. E. *Kinetics of Precipitation*; Pergamon: Oxford, U.K., 1964.

$$\Delta G^* = B\left(\frac{k_B T}{\sigma^2}\right) \quad (3)$$

such that components of ΔG^* (excluding supersaturation) may be grouped into a shape-specific constant B,[35] which we determined directly from the experimental surface nucleation rates without direct knowledge or assumption of nucleus shape (see Supporting Information). Combining eqs 2 and 3 and then rewriting into linear form gives

$$\ln J_n = \ln A - B\left(\frac{1}{\sigma^2}\right) \quad (4)$$

where the slope, B, is directly proportional to the energy barrier to surface nucleation and the intercept, ln A, contains kinetic factors that govern nucleation frequency.

Fitting eq 4 to the data shows that silica nucleation rates onto NH_3^+/COO^-- and COO^--functionalized substrates exhibit a linear dependence on $1/\sigma^2$ as predicted by nucleation theory (Figure 4). Rates measured for the NH_3^+/COO^- substrates are approximately 18× faster than those observed for COO^- surfaces for driving forces where surface-promoted nucleation occurs (e.g., Figure 4). However, both surface types exhibit similar dependencies on chemical driving force σ. That is, the data show that nuclei forming on both types of substrates have similar shape factors ($B = 39.4 \pm 13.3$ and 37.6 ± 6.2 for NH_3^+/COO^- and COO^- substrates, respectively) and that nucleation on these substrates proceeds against similar thermodynamic barriers (eq 3). The faster nucleation rates onto NH_3^+/COO^- surfaces arise, therefore, from increases in factors contained within A (values of ln A measured for the carboxyl and hybrid surfaces are 27.1 ± 1.6 and 30.0 ± 3.3, respectively). While there is some calculated uncertainty in the measured values of ln A, observations of patterned surfaces (e.g., Figure 3) provide independent evidence for faster rates on hybrid surfaces. Although theory allows for nucleation to be influenced by both thermodynamic and kinetic drivers (e.g., ΔG^* and ln A), the reduction in the height of the free energy barrier to nucleation is generally assumed to be the dominant factor controlling the rate of surface nucleation. However, at least for silica nucleation, kinetic drivers appear to be sensitive enough to the nature of the organic template to cause significant variations in the surface nucleation rate between substrates.

Origins of Kinetic Factors in Governing Nucleation Rates. Surface-assisted nucleation can occur only when the height of the thermodynamic barrier to nucleation at the surface is less than in solution. In the present study, we determined that the surface-induced reduction in the nucleation barrier is essentially the same for both COO^- and NH_3^+/COO^- substrates. Therefore, the ~18-fold offset in the nucleation rate presumably reflects differences in the density of favorable sites for nucleation and kinetic processes that occur on these substrates during silica formation. Because solution-flow rates used in this study were adjusted to ensure that nucleation was limited by surface kinetics rather than bulk diffusion, the most likely sources of kinetic variability are (1) differential modulation of steric barriers and molecular-level attachment kinetics through surface-directed structuring or orientation of silicic acid adsorbates and (2) substrate specific differences in the local concentration and ratio of neutral to ionized silicic acid surface species. Both scenarios would directly affect the frequency factor, A, contained within eq 4 without requiring any significant or experimentally quantifiable reduction in the free energy barrier to surface nucleation.

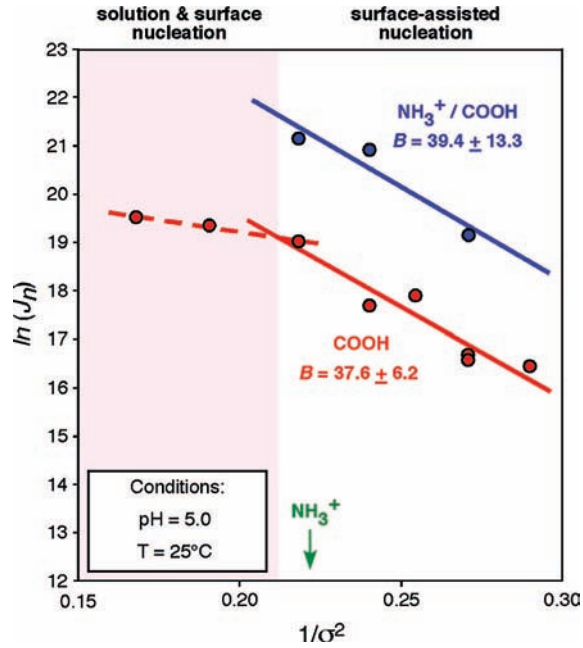

Figure 4. Plot showing the natural log of the substrate-specific nucleation rate versus the inverse square of supersaturation at pH = 5.0 and $T = 25$ °C. The nucleation field exhibits two regions where (1) nucleation occurs concomitantly on the surface and in solution, and (2) silica nucleation occurs exclusively on the surface. In the surface-assisted nucleation regime, the slope of the trend line yields B, which is directly proportional to the work of nucleus formation ΔG^*.

The inability of aminated substrates to direct the formation of amorphous silica nuclei without accompanying anionic species apparently results from inhibited kinetic pathways, high free energy barriers to nucleation on these surfaces, or the combined effects thereof. Because the magnitude of ΔG^* is determined from nucleation rate data, and because silica did not form on the amine-terminated surfaces, the height of the free energy barrier to nucleation on these substrates cannot be quantified at this time. Therefore, to what degree the NH_3^+ surface passivity is caused by thermodynamic versus kinetic drivers remains uncertain. The most likely source is ΔG^*, which, as a result of its cubic dependence upon the liquid−substrate interfacial energy γ_{ls}, dominates the nucleation rate equation as the argument of an exponential term (see derivation in Supporting Information). Note that A also contains an exponential term, but it is comparatively insensitive to small changes in γ_{ls}.

Conclusions and Implications

Thermodynamic and kinetic barriers to silica nucleation were determined from kinetic measurements on amine-, carboxyl-, and hybrid NH_3^+/COO^--terminated surfaces under chemical conditions similar to those inferred from natural biosilica deposition environments. The fastest rates were measured on the hybrid surfaces and were ~18× greater than the rate of silica nucleation on carboxyl-terminated surfaces under comparable conditions. The energy barriers to silica nucleation on these two surface types were also determined to be similar, suggesting that surface nucleation rates are more sensitive to kinetic drivers than anticipated. The aminated substrates were initially resistant to silica deposition, and therefore, the surface nucleation rate could not be obtained. However, subsequent experiments with patterned NH_3^+- and COO^--terminated domains and solution-borne phosphate anions showed that ami-

nated surfaces do facilitate silica formation if anionic species are proximal. This result indicates that cooperative interactions arising between adjacent chemical moieties on silica-mineralizing organic templates are critical for controlling the rate and locus of silica formation. It also speaks to the concept that supramolecular assemblies of biomolecules express emergent properties that accelerate mineral formation to a degree that is not attainable by their individual molecular constituents.

Implications for Silica Biomineralization. These findings suggest that current explanations for the roles of aminated compounds in silica biomineralization may need to be expanded to consider the functions that neighboring anionic species may assume during silica nucleation. To date, most theoretical and experimental studies of silica biomineralization have focused on the seemingly intrinsic ability of aminated compounds to promote the hydrolysis of organosilicate precursors to silicic acid,[18,21−23,28,38−52,54] and to direct the aggregation of oligomeric silicic acid species. The evidence supporting this interpretation comes largely from the zeolite synthesis literature,[28,55] where aminated compounds facilitate the formation of complex silicate structures under extreme conditions of high pH, supersaturation, and sometimes temperature. For the comparatively mild conditions used in this study, which were chosen to approximate the conditions found in natural silica biomineralization environments, the presence of anionic groups is prerequisite for silica deposition upon aminated surfaces. Again this suggests that the role of aminated compounds in conferring activity for silica nucleation during biomineralization relies at the very least upon the proximity of an anionic or ionizable group, such as serine in the active site of silicatein-type sponge spicule proteins.

Insights from this study also provide means for better understanding the activity of macromolecules implicated in diatom mineralization. For example, diatom silaffin proteins are characterized by specific modifications to lysine and serine residues within the peptide backbone. The lysine residues possess elongated alkane chains, punctuated by amine moieties in varying states of protonation [18,19] while serine residues are typically phosphorylated and negatively charged under physiological conditions.[20] Silacidin proteins are chemically similar to the amine-rich silaffins but without the lysine side chains.[56] Investigations employing these macromolecules[18−22,56] and structural analogues thereof[17,22,26,27,29,37−41,43,44,50−52,57−64] argue that electrostatic attractions between oppositely charged sites on silaffins, silacidins, polyamines, and/or solution-borne anions trigger the phase separation and self-assembly of these macromolecules into an organic matrix, which presumably acts as a structural template for silica deposition within specialized silica deposition vesicles (SDV).[17,20−22,26,29,37,59,64] Our findings suggest that the cooperative electrostatic interactions underlying formation of the organic matrix also control the spatial onset of silica formation within it. That is, sites on the organic matrix that have anionic species such as carboxyl or phosphoryl groups in close proximity to amine moieties could be likely points of initial silica deposition. While the detailed mechanism by which the organic matrix acts to initialize and promote silica mineralization is as yet unknown, it is clear that macromolecular assemblies possess emergent properties that can strongly influence mineral formation in biomimetic systems. These observations open intriguing new questions for further experimental study into this newly recognized type of emergent behavior.

Evidence for silica mineralization promoted by the synergistic activity of proximal cationic and anionic groups also suggests a plausible explanation for how microbial surfaces can facilitate silica mineralization. For example, under certain circumstances, microbially produced extracellular polymeric substances may create local environments for silica deposition that closely resemble the chemical conditions within diatom silica deposition vesicles. Along these lines, it has been suggested that silica mineralization on cell membranes, as found in hydrothermal environments,[65−67] could be promoted by the adsorption of microbially produced polyamines to negatively charged extracellular polymeric substances (EPS) on the outer cell surface.[67,68] Similar types of chemical interactions may also influence the postmortem preservation of microbes and other organic-walled microfossils.[69−72] For example, it has been shown that mineralization onto decaying plant matter with a rich EPS coating is favored over the same fresh material.[73] This would suggest that the degree of preservation could be an indicator of the chemical nature of these biological substrates during the early stages of fossilization.

Insights for Surface-Assisted Nucleation. Surface nucleation is driven primarily by local fluctuations in the interfacial energy, which manifest themselves as reductions in the thermodynamic barrier to cluster formation specifically at the solution−substrate interface. The ability of a given substrate to accelerate the surface-assisted nucleation rate is generally attributed to the magnitude of the free energy reduction. Contributions to nucleation rates that arise from consideration of kinetic processes are usually estimated and assumed to be negligible with respect to what are presumably much more consequential thermodynamic drivers. However, our findings demonstrate that, in the case of silica nucleation, variations in the pre-exponential kinetic factor A can cause marked variations in the surface nucleation rate between substrates (up to $\sim 18\times$), without requiring a significant concomitant reduction in the thermodynamic barrier to critical cluster formation. These new insights into the relative

(54) Delak, K. M.; Sahai, N. *J. Phys. Chem. B* **2006**, *110*, 17819–17829.
(55) Davis, M. E.; Lobo, R. F. *Chem. Mater.* **1992**, *4*, 756–768.
(56) Wenzl, S.; Hett, R.; Richthammer, P.; Sumper, M. *Angew. Chem., Int. Ed.* **2008**, *47*, 1729–1732.
(57) Roth, K. M.; Zhou, Y.; Yang, W. J.; Morse, D. E. *J. Am. Chem. Soc.* **2005**, *127*, 325–330.
(58) Knecht, M. R.; Wright, D. W. *Langmuir* **2004**, *20*, 4728–4732.
(59) Groger, C.; Lutz, K.; Brunner, E. *Cell Biochem. Biophys.* **2008**, *50*, 23–39.
(60) Belton, D. J.; Patwardhan, S. V.; Perry, C. C. *J. Mater. Chem.* **2005**, *15*, 4629–4638.
(61) Helmecke, O.; Hirsch, A.; Behrens, P.; Menzel, H. *J. Colloid Interface Sci.* **2008**, *321*, 44–51.
(62) Menzel, H.; Horstmann, S.; Behrens, P.; Barnreuther, B.; Krueger, I.; Jahns, M. *Chem. Commun.* **2003**, 2994–2995.
(63) Patwardhan, S. V.; Clarson, S. J.; Perry, C. C. *Chem. Commun.* **2005**, 1113–1121.
(64) Sumper, M.; Brunner, E. *Adv. Funct. Mater.* **2006**, *16*, 17–26.
(65) Konhauser, K. O.; Phoenix, V. R.; Bottrell, S. H.; Adams, D. G.; Head, I. M. *Sedimentology* **2001**, *48*, 415–433.
(66) Konhauser, K.; Jones, B.; Phoenix, V.; Ferris, G.; Renaut, R. *Ambio* **2004**, *33*, 552–558.
(67) Lalonde, S. V.; Konhauser, K.; Reysenbach, A. L.; Ferris, F. G. *Geobiology* **2005**, *3*, 41–52.
(68) Furukawa, Y.; O'Reilly, S. E. *Geochim. Cosmochim. Acta* **2007**, *71*, 363–377.
(69) Westall, F. *J. Geophys. Res., [Planets]* **1999**, *104*, 16437–16451.
(70) Kempe, A.; Schopf, J. W.; Altermann, W.; Kudryavtsev, A. B.; Heckl, W. M. *Proc. Natl. Acad. Sci. U.S.A.* **2002**, *99*, 9117–9120.
(71) Reysenbach, A. L.; Cady, S. L. *Trends Microbiol.* **2001**, *9*, 79–86.
(72) Knoll, A. H.; Strother, P. K.; Rossi, S. *Precambrian Res.* **1988**, *38*, 257–279.
(73) Dunn, K. A.; McLean, R. J. C.; Upchurch, G. R.; Folk, R. L. *Geology* **1997**, *25*, 1119–1122.

importance of kinetic and thermodynamic drivers of surface nucleation merit further study and suggest that new bioinspired approaches to silica-based materials synthesis may be feasible. In particular, the emergent properties of the self-assembled mineralization template may be exploited to control the nucleation, growth, and morphology of mineral phases with a degree of fidelity that is currently achieved only by living organisms.

Experimental Section

Substrate Preparation. Evaporated gold on mica substrates obtained from Agilent Technologies was used to produce ultraflat Au(111) surfaces by the template-stripped gold method.[74] Chemically uniform carboxyl- and amine-terminated surfaces were produced by immersing the freshly cleaved gold substrates in 1 mM ethanol-based solutions (200 proof anhydrous, Sigma Aldrich) of 11-mercaptoundecanoic acid (MUA; 95%, Sigma Aldrich) and 11-amino-1-undecanethiol hydrochloride (AUT; 99%, Dojindo Molecular Technologies) for no less than 24 h at room temperature. Mixed surfaces containing both carboxyl and amine moieties were also produced by this method, but the composition of the ethanol solution was adjusted to be 1 mM with respect to both MUA and AUT. Because MUA and AUT have the same alkyl chain length, phase separation on these surfaces was minimal, and relatively homogeneous substrates were produced.

Chemically patterned surfaces with alternating stripes of MUA and AUT were produced with microcontact soft lithography.[75] Carboxyl-terminated stripes were deposited by bringing an MUA-coated polydimethylsiloxane (PDMS) polymer stamp into contact with the Au(111) surface for 10−15 s. Those regions of the gold substrate left bare after the stamping procedure were functionalized with amine moieties by immersing the stamped gold substrate in a 10 mM ethanolic solution of AUT for 20 min. All substrates were thoroughly rinsed with ethanol and water before use.

Preparation of Solutions. For nucleation studies, organic precursors to H_4SiO_4 are preferable to traditional sodium silicate sources because the resulting solutions are free of polysilicic acids and supercritical clusters of SiO_2 at the outset of the experiment. Sodium silicate solutions are problematic because they generally contain a small but significant population of condensed silicate species.[76] Acid-catalyzed hydrolysis of silicon alkoxides, such as tetramethyl orthosilicate (TMOS), is rapid and nearly complete at low pH and high water-to-silicon ratios[77,78] and produces only monomeric silicon species and methanol as byproducts. Supersaturated silicic acid solutions were prepared immediately before the start of each experiment by adding a prescribed amount of TMOS (99.5+%, Sigma Aldrich) to a dilute hydrochloric acid solution at pH $\approx$ 2.0. The pH of these solutions was adjusted to pH = 5.0 (the experimentally determined pH of the silica deposition environment in diatoms[79]) by adding an equal volume of NaOH/NaCl solution. The resulting solutions contained 0.1 mol/L NaCl (99.9999%, Sigma Aldrich) as background electrolyte and variable, but predetermined and controlled, concentrations of H_4SiO_4. The stability of these solutions was determined by the molybdate yellow method, which measures the concentration of low molecular weight silicic acid polymers (monomers, dimers, and trimers) in solution. At $\sigma \leq 2.14$ these solutions had a 2−3+ h induction time to solution nucleation. Above $\sigma = 2.14$, the induction time decreased and was ~45−60 min at $\sigma = 2.44$. All surface nucleation rate measurements (see below) were obtained in the time interval before the onset of solution nucleation. Some experiments also contained 5 mM orthophosphate, which was added as dibasic sodium phosphate (99.99%, Fluka); consequently, the concentration of Na in solution was also increased by 10% to 0.11 mol/L in experiments that contained the phosphate anion.

Nucleation Rate Measurements. Substrate-specific nucleation rates were measured by tracking the increase in the number of silica nuclei per unit area of surface as a function of time with tapping-mode atomic force microscopy (TM-AFM). The use of tapping mode is paramount in these experiments because the forces arising from interactions between the surface and AFM tip are minimized and are far less likely to displace developing nuclei and to influence interfacial processes than contact-mode AFM. To ensure steady-state conditions, growth solutions were pumped through the AFM flow cell at a constant rate of 30 mL/h at ambient temperature, an environment that has been previously shown to produce non-diffusion-limited conditions for calcite growth.[80] Measurements were made over a range of chemical driving force or supersaturation (eq 1). Nucleation rate measurements were determined from data collected shortly after the onset of silica deposition, where the increase in silica particle density exhibited a linear dependence on time. Data used in our analyses were typically obtained within the first 1−2 h of each experiment and always within the time frame defined by the induction time to solution nucleation (2−3+ h at $\sigma \leq 2.14$).

Acknowledgment. This material is based upon work supported by the National Science Foundation (EAR-0545166) and the Department of Energy (FG02-00ER15112). This work was also performed under the auspices of the U.S. DOE by award to J.J.D. at the University of California, Lawrence Livermore National Laboratory, under Contract W-7405-Eng-48. Additionally, we thank J. Don Rimstidt for providing helpful comments on the manuscript.

Supporting Information Available: Documentation of the theoretical basis underlying the determination of silica−substrate contact angles from experimentally determined surface nucleation rates. This material is available free of charge via the Internet at http://pubs.acs.org.

JA809486B

(74) Hegner, M.; Wagner, P.; Semenza, G. *Surf. Sci.* **1993**, *291*, 39–46.
(75) Wilbur, J. L.; Kumar, A.; Kim, E.; Whitesides, G. M. *Adv. Mater.* **1994**, *6*, 600–604.
(76) Felmy, A. R.; Cho, H.; Rustad, J. R.; Mason, M. J. *J. Solution Chem.* **2001**, *30*, 509–525.
(77) Tejedor-Tejedor, M. I.; Paredes, L.; Anderson, M. A. *Chem. Mater.* **1998**, *10*, 3410–3421.
(78) Assink, R. A.; Kay, B. D. *J. Non-Cryst. Solids* **1988**, *99*, 359–370.
(79) Vrieling, E. G.; Gieskes, W. W. C.; Beelen, T. P. M. *J. Phycol.* **1999**, *35*, 548–559.
(80) Teng, H. H.; Dove, P. M.; Orme, C. A.; De Yoreo, J. J. *Science* **1998**, *282*, 724–727.